Journal of Ceramic Processing Research. Vol. 13, No. 3, pp. 291~295 (2012)

J O U R N A L O F
Ceramic Processing Research

MAS synthesis and characterization of $Sr_3V_2O_8$ nanoparticles

Kwang Bo Shim[a] and Chang Sung Lim[b,*]

[a]*Division of Materials Science and Engineering, Hanyang University, Seoul 133-791, Korea*
[b]*Department of Advanced Materials Science & Engineering, Hanseo University, Seosan 356-706, Korea*

$Sr_3V_2O_8$ nanoparticles were synthesized successfully using a MAS (microwave-assisted solvothermal) route followed by further heat-treatment. Well-crystallized $Sr_3V_2O_8$ nanoparticles were formed after heat-treatment at 600 °C for 3 h showing a fine and homogeneous morphology with particle sizes of 100-150 nm. The synthesized $Sr_3V_2O_8$ nanoparticles were characterized by X-ray diffraction, Fourier transform infrared spectroscopy, scanning electron microscopy, energy-dispersive X-ray spectroscopy and transmission electron microscopy. The optical properties were investigated by photoluminescence emission and Raman spectroscopy.

Key words: $Sr_3V_2O_8$, MAS, Nanoparticles, Luminescence, Raman spectroscopy.

Introduction

Metal orthovanadates have attracted considerable attention for potential applications in photoluminescence, IR-laser, light-emitting diode, photocatalyst, ferroelectric and microwave devices [1-3]. The physical, chemical and photochemical properties of metal orthovanadates are dependent on the manufacturing method. Several processes have been developed over the past decade to enhance the applications of $Sr_3V_2O_8$ prepared by a range of processes, such as a solid-state reaction [4, 5], a solution phase metathetic method [6], a sol-gel method [7], a solid-state metathesis approach [8], a mechano-chemical method [9] and a floating zone technique [10]. Among these methods, solution-based chemical synthetic methods play a key role in the design and production of fine ceramics and have been successful in overcoming many of the limitations of traditional solid-state, high-temperature methods. Compared with the usual methods, microwave synthesis has the advantages of a very short reaction time, a small particle size, a narrow particle size distribution, and is a high purity method for preparing polycrystalline samples. Microwave heating is delivered to the surface of the material by radiant and/or convection heating, which is transferred to the bulk of the material via conduction. Microwave energy is delivered directly to the material through molecular interactions with an electromagnetic field. Heat can be generated through volumetric heating because microwaves can penetrate the material and supply energy [11].

A hydrothermal process is an efficient low temperature method which allows the formation of particles with a high degree of crystallinity and easy dispersion in an aqueous medium. The use of microwave energy in a hydrothermal system promotes the development of a rapid heating to the required temperature with rapid rates of crystallization [12, 13]. Recently, Fu et al. [14] and Thongtem et al. [15] have been reported the use of a fast method in preparing nanocrystalline particles of metal tungstates with unique and enhanced properties by a MAS(microwave-assisted solvothermal) process. A solvothermal process is one of the most powerful method employed for the crystallization of various unique nanoparticles. The solvothermal process is the reaction of a hot solution within or on the surface of a substance. Ethylene glycol, as a polar solvent with a boiling point of 197 °C, is a good candidate for the MAS process. When the solvent is ethylene glycol, the reactions proceed in a sealed pressure autoclave at temperatures of the boiling point of the ethylene glycol. The microwave radiation is supplied to the ethylene glycol, so that the components dissolving in the ethylene glycol are capable of coupling with radiation. When a large amount of microwave radiation is applied into the ethylene glycol under a high sealed pressure, the charged particles are vibrated in the electric field interdependently. Therefore, it is possible to achieve rapid and uniform heating of microwave dielectric materials. A MAS process using a solvent of ethylene glycol is a convenient process that provides a high-qualified yield with cost-effective method in short time periods.

However, the study of the MAS process of $Sr_3V_2O_8$ nanoparticles has not been published previously. Therefore, the precise nature of the optical properties and the MAS process of $Sr_3V_2O_8$ nanoparticles are required for a wide range of applications. In this study,

*Corresponding author:
Tel : +82-41-660-1445
Fax: +82-41-660-1445
E-mail: cslim@hanseo.ac.kr

the $Sr_3V_2O_8$ nanoparticles were synthesized using a MAS route. The characteristics of the synthesized $Sr_3V_2O_8$ nanoparticles are discussed in detail based on the MAS reaction in ethylene glycol under the high sealed pressure. The synthesized $Sr_3V_2O_8$ nanoparticles were characterized by X-ray diffraction (XRD), Fourier transform infrared spectroscopy (FTIR), scanning electron microscopy (SEM), energy-dispersive X-ray spectroscopy (EDS) and transmission electron microscopy (TEM). The optical properties were examined by photoluminescence (PL) emission and Raman spectroscopy.

Experimental

Fig. 1 shows a flow chart for the synthesis of $Sr_3V_2O_8$ nanoparticles by the MAS process. $SrCl_2 \cdot 6H_2O$, Na_3VO_4 and ethylene glycol of analytic reagent grade (Aldrich) were used to prepare the $Sr_3V_2O_8$ compound. Each of 0.012 mol $SrCl_2 \cdot 6H_2O$ and 0.008 mol Na_3VO_4 was dissolved in 30 ml ethylene glycol. The solutions were mixed and adjusted to a pH 9.5 using NaOH. The aqueous solution was stirred in an ultrasonic bath at room temperature. In the sequence, the mixture was transferred into a Teflon-lined digestion vessel of 120 ml capacity. The Teflon vessel was placed into a MAS oven (2.45 GHz, maximum power of 800 W). The MAS conditions were kept at 200 °C for 23 minutes. After MS process, the MAS oven was cooled to room temperature. The resulting solutions were treated with ultrasonic radiation and washed many times with distilled hot water. The white precipitates were collected and dried at 100 °C in a dry oven. The final products were heat-treated at 600 °C for 3 h.

The existing phases of the $Sr_3V_2O_8$ particles after the MAS process were identified by powder XRD (CuK_α, Rigaku D/MAX 2200, Japan). FTIR (Nicolet IR 200, Thermo Electron Corporation, USA) was used to examine the absorption behavior of the synthesized

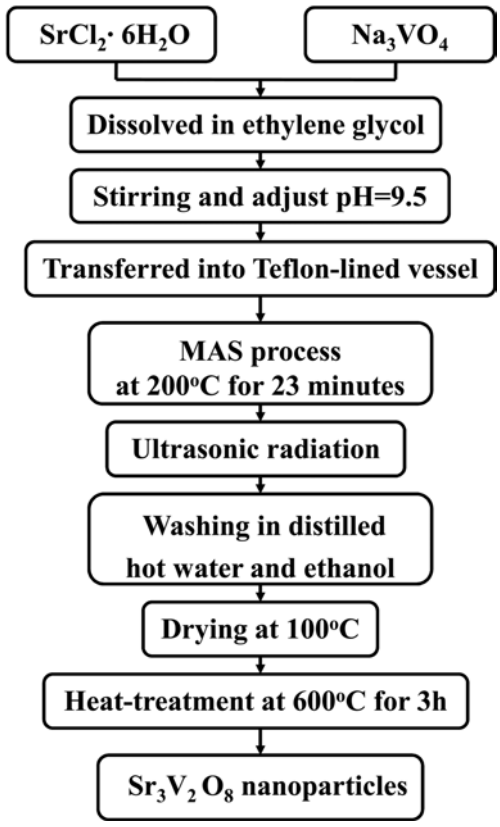

Fig. 1. Flow chart for the synthesis of $Sr_3V_2O_8$ nanoparticles by the MAS process.

$Sr_3V_2O_8$ particles over the frequency range, 400 to 4000 cm^{-1}. The microstructure, particle morphology and qualitative compositions of the $Sr_3V_2O_8$ particles were observed by SEM (JSM-5600, JEOL, Japan), EDS and TEM (JEM 2000-FX, 250 kV, Japan). The PL spectra were recorded using a spectrophotometer (Perkin Elmer LS55, UK) at room temperature. Raman spectroscopy measurements were performed using LabRam HR (Jobin-Yvon, France). The 514.5 nm line

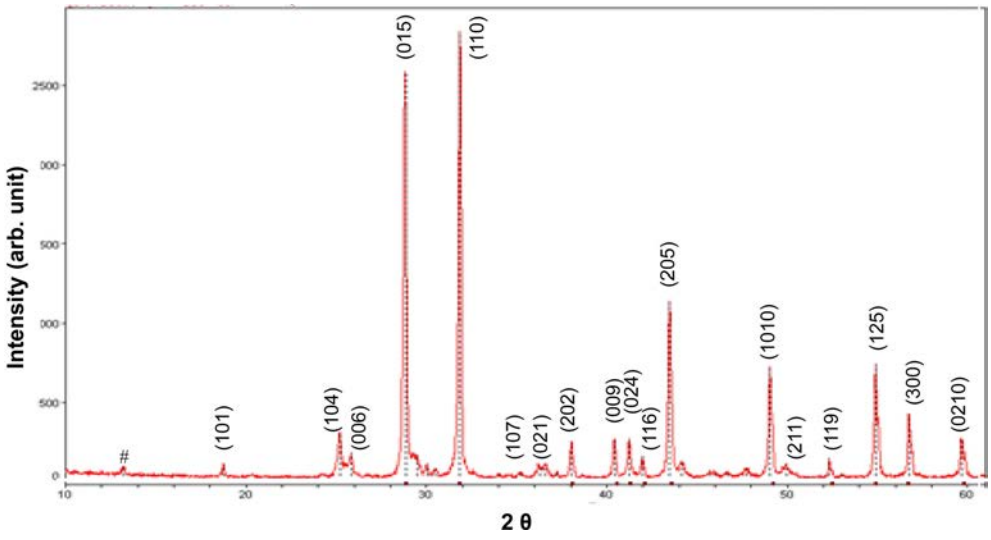

Fig. 2. XRD pattern of the synthesized $Sr_3V_2O_8$ nanoparticles.

of an Ar-ion laser was used as the excitation source, the power was kept at 0.5 mW on the samples.

Results and discussion

Fig. 2 shows an XRD pattern of the synthesized $Sr_3V_2O_8$ nanoparticles. All observed diffraction peaks could be assigned to the trigonal phase (space group *R-3 m*), which is in good agreement with the crystallographic data of $Sr_3V_2O_8$ (JCPDS: 81-1844) [8]. This means that the trigonal phases of $Sr_3V_2O_8$ can be prepared using this MAS. This suggests that MAS synthesis is suitable for the growth of $Sr_3V_2O_8$ crystallites and the development of the strongest intensity peaks from the (015), (110) and (205) planes, which were the major peaks of the $Sr_3V_2O_8$, with some preferred orientation. A small amount of NaCl marked with # at 13.2 ° was observed. The MAS process occurs in accordance with the reaction : $3SrCl_2 \cdot 6H_2O + 2Na_3VO_4 \rightarrow Sr_3V_2O_8 + 6NaCl + 18H_2O$. The presence of the residual NaCl resulted from this solvothermal reaction.

Fig. 3 shows a SEM image (a) and a TEM image (b) of the syntheisized $Sr_3V_2O_8$ nanoparticles. The SEM image of $Sr_3V_2O_8$ in Fig. 3(a) shows a well-defined and homogeneous morphology, while the TEM image of $Sr_3V_2O_8$ in Fig. 3(b) shows the particle sizes of 100-150 nm. The MAS synthesis proceeds the reaction of $SrCl_2 \cdot 6H_2O + Na_3VO_4$ in a hot ethylene glycol solution as a polar solvent with a boiling point of 197 °C. When the microwave radiation is supplied to the ethylene glycol under a sealed pressure at the boiling point, the components dissolving in the ethylene glycol are charged and vibrated in the electric field interdependently. The MAS process is adjusted to heat the metal orthovanadates uniformly

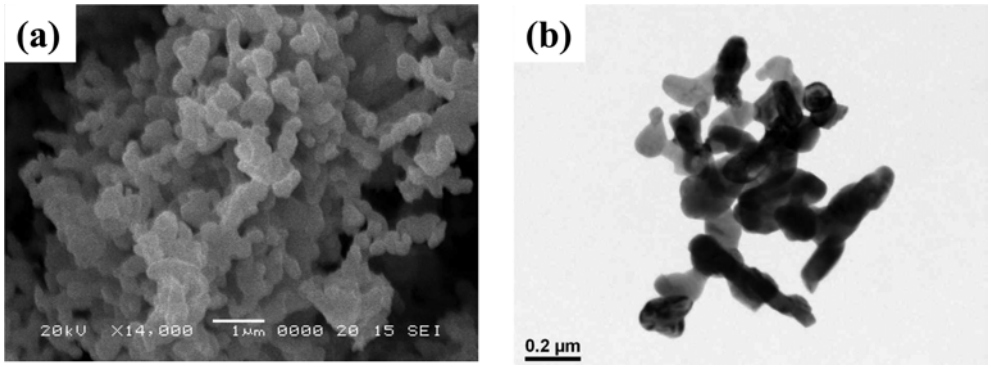

Fig. 3. A SEM image (a) and a TEM image (b) of the synthesized $Sr_3V_2O_8$ nanoparticles.

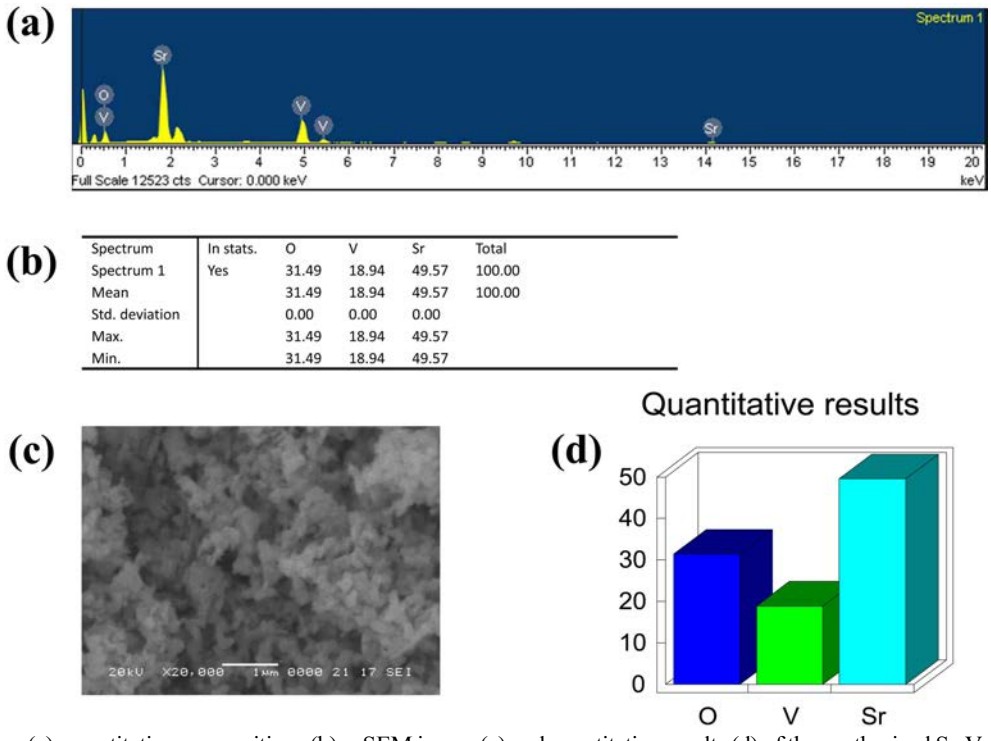

Fig. 4. EDS pattern (a), quantitative compositions (b), a SEM image (c) and quantitative results (d) of the synthesized $Sr_3V_2O_8$ nanoparticles.

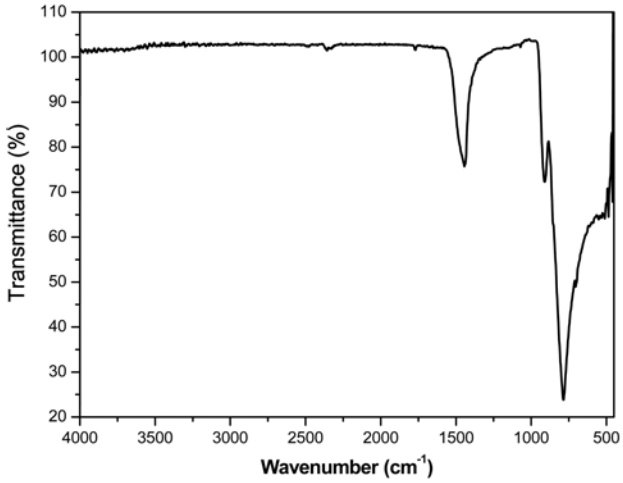

Fig. 5. FT-IR spectrum of the synthesized $Sr_3V_2O_8$ nanoparticles.

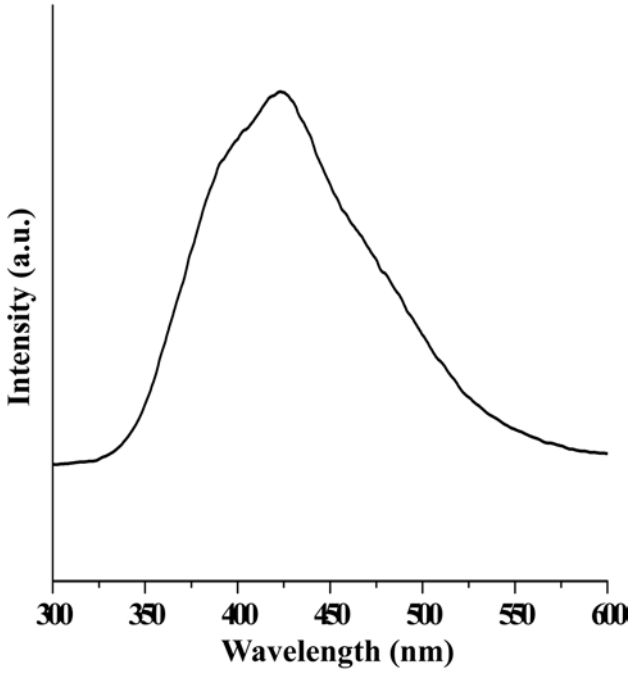

Fig. 6. PL emission spectrum of the synthesized $Sr_3V_2O_8$ nanoparticles excited at 250 nm at room temperature.

resulting in fine particles with a controlled morphology, and to fabricate the product in a green manner without the generation of solvent waste. The MAS reaction involves the exchange of atomic/ionic species, where the driving force is the exothermic reaction in ethylene glycol accompanying the formation of NaCl with a high lattice energy. The MAS reaction occurs so rapidly that the temperature and the pressure of the ethylene glycol increases so quickly that the reaction products are essentially heated up. The MAS reactions provide a convenient route for the synthesis of $Sr_3V_2O_8$ nanoparticles at considerably lower temperatures with a high pressure than those usually employed for their synthesis. The well-defined $Sr_3V_2O_8$ nanoparticle features synthesized by the MAS process have a control over the

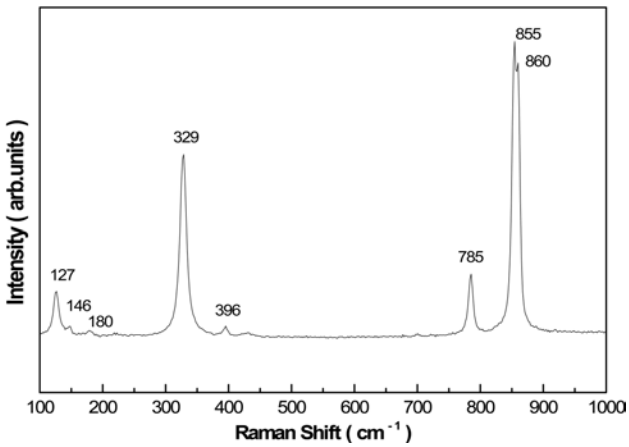

Fig. 7. Raman spectrum of the synthesized $Sr_3V_2O_8$ nanoparticles excited by the 514.5 nm line of an Ar-ion laser at 0.5 mW on the samples.

morphology of the final particles, and can be used for technological applications.

Fig. 4 shows an EDS pattern (a), quantitative compositions (b), a SEM image (c) and quantitative results (d) of the synthesized $Sr_3V_2O_8$ nanoparticles. The EDS pattern and quantitative compositions in Fig. 4 (a, b) could be assigned to $Sr_3V_2O_8$. This means that the $Sr_3V_2O_8$ can be successfully synthesized using this MAS process. The quantitative results of the morphology in Fig. 4(c, d) were composed of Sr, V and O.

Fig. 5 shows an FT-IR spectrum of the syntheisized $Sr_3V_2O_8$ nanoparticles in the wavenumber range, 480-4000 cm^{-1}. The large isolated absorbable peak around 820 cm^{-1} reveals a typical characteristic of a strong V-O stretching in the $[VO_4]^{3-}$ with a strong IR absorbing band at 920 cm^{-1}. The strong V-O stretching peaks contribute to the uniform regular $[VO_4]^{3-}$ tetrahedron of the metal orthovanadates.

Fig. 6 shows a PL emission spectrum of the synthesized $Sr_3V_2O_8$ nanoparticles excited at 250 nm at room temperature. The emission spectra of metal orthovanadates are due mainly to charge-transfer transitions within the $[VO_4]^{3-}$ complex. With excitation at 250 nm $Sr_3V_2O_8$ nanoparticles exhibit major PL emissions in the blue wavelength range of 420-430 nm. The spectrum shows broad peaks on which are superimposed considerable several fine structures.

Fig. 7 shows the Raman spectrum of the $Sr_3V_2O_8$ nanoparticles excited by the 514.5 nm line of an Ar-ion laser kept at a power of 0.5 mW on the samples. The vibration modes in the Raman spectra of $Sr_3V_2O_8$ nanoparticles are classified into two groups, internal and external. The internal vibrations are related to the $[VO_4]^{3-}$ molecular group with a stationary mass center. The external vibrations or lattice phonons are associated to the motion of the Sr^{2+} cation and rigid molecular units. The Raman modes for the $Sr_3V_2O_8$ nanoparticles were detected as $\nu_1(A_g)$, $\nu_3(B_g)$, $\nu_3(E_g)$, $\nu_4(E_g)$, $\nu_4(B_g)$ and $\nu_2(B_g)$ vibrations at 860, 855, 785,

396 and 329 cm^{-1}, respectively. The free rotation mode was detected at 180 cm^{-1} and the external modes were localized at 146 and 127 cm^{-1}. The well-resolved sharp peaks for the $Sr_3V_2O_8$ nanoparticles indicate that the synthesized particles are highly crystallized.

Conclusions

$Sr_3V_2O_8$ nanoparticles were synthesized successfully using a MAS route in a hot ethylene glycol solution as a polar solvent. Well-crystallized $Sr_3V_2O_8$ nanoparticles were formed after heat-treatment at 600 °C for 3 h showing a fine and homogeneous morphology with particle sizes of 100-150 nm. With excitation at 250 nm, the $Sr_3V_2O_8$ exhibit major PL emissions in the blue wavelength range of 420-430 nm. The Raman modes for the $Sr_3V_2O_8$ nanoparticles were detected at 860, 855, 785, 396 and 329 cm^{-1}, the free rotation mode was detected at 180 cm^{-1} and the external modes were localized at 146 and 127 cm^{-1}. The well-resolved sharp peaks for the $Sr_3V_2O_8$ nanoparticles indicate that the synthesized particles are highly crystallized.

Acknowledgement

This study was supported by Basic Science Research Program through the National Research Foundation of Korea (NRF) funded by the Ministry of Education, Science and Technology (2011-0026911).

References

1. T. Nakajima, M. Isobe, T. Tsuchiya, Y. Ueda, T. Kumagai, J. Luminescence 129 (2009) 1598-1601.
2. F. Yen, R.P. Chaudhury, E. Galstyan, B. Lorenz, Y.Q. Wang, Y.Y. Sun, C.W. Chu, Physica B 403 (2008) 1487-1489.
3. N. Rogado, G. Lawes, D.A. Huse, A.P. Ramirez, R.J. Cava, Solid State Comm. 124 (2002) 229-233.
4. D. Wang, Z. Zou, J. Ye, Res. Chem. Intermed. 31 (2005) 433-439.
5. M. Kurzawa, A. Blonska-Tabero, J. Therm. Anal. Calorim. 77 (2004) 17-24.
6. P. Parhi, V. Manivannan, Mat. Res. Bull. 43 (2008) 2966-2973.
7. S.S. Kim, H. Ikuta, M. Wakihara, Solid State Ionics 139 (2001) 57-65.
8. P. Parhi, V. Manivannan, S. Kohli, P. Mccurdy, Bull. Mater. Sci. 31 (2008) 885-890.
9. V. Manivannan, P. Parhi, J. Howard, J. Cry. Growth 310 (2008) 2793-2799.
10. R. Szymczak, M. Baran, J. Fink-Finowicki, B. Krzymanska, P. Aleshkevych, H. Szymczak, S.N. Barilo, G.L. Bychkov, S.V. Shiryaev, J. Non-Crystalline Solids 354 (2008) 4186-4188.
11. S. Das, A.K. Mukhopadhyay, S. Datta, D. Basu, Bull. Mater. Sci. 32 (2009) 1-13.
12. K.P.F. Siqueira, R.L. Moreira, M. Valadares, A. Dias, J. Mat. Sci. 45 (2010) 6083-6093.
13. J.C. Sczancoski, L.S. Cavalcante, M.R. Joya, J.a. Varela, P.S. Pizani, E. Longo, Chemical Eng. J. 140 (2008) 632-637.
14. J. Bi, L. Wu, Z. Li, Z. Ding, X. Wang, X. Fu, J. Alloys & Comp. 480 (2009) 684-688.
15. T. Thongtem, A. Phuruangrant, S. Thongtom, Curr. Appl. Phy. 8 (2008) 189-197.